Planning Stable Trajectory on Uneven Terrain based on Feasible Acceleration Count

Arun Kumar Singh, K.Madhava Krishna and Vijay Eathakota

Abstract—**In this paper we propose a novel physics based motion planning and trajectory generation framework for vehicle operating on uneven terrains. The proposed framework provides for a fully 3D analysis of the dynamic constraints of the vehicle on uneven terrain and hence comes as a better approach than the existing motion planning framework which makes simplifying assumptions for the terrain conditions or the vehicle geometry or both. The entire framework consists of three major parts which are: 1. A framework for determination of the posture of a vehicle in 3D for a given terrain. 2. A framework for determination of maximum feasible velocities and acceleration based on contact and no-slip constraints. 3. Combining the above two framework to generate feasible trajectories for the vehicle. Trajectories are generated through a Dynamic Window paradigm extended to fully 3D terrains, wherein the next best node is selected through a new metric that maximizes the space of feasible velocities and accelerations and reduces the distance to be traversed to the goal**

I. INTRODUCTION

With the advent of outdoor robotics and as more and more robots operate outdoors they are entailed to navigate on terrains that are uneven. This requires some paradigm changes in the way path planning algorithm needs to operate. Unlike indoors where obstacles are vertical projections from a horizontal ground plane and all obstacles need to be strictly avoided, in outdoors the distinction between obstacles and ground is hazy as the obstacles and ground blend with each other to form the terrain. Thus one is required to go beyond usual geometric and kinematic path finding algorithms towards algorithms that integrate notions of terrain traversability into their path planning or path finding procedures.

One of the popular methods of ascertaining terrain traversability is through the tipover stability margin introduced in [1] and modified to account for changing vehicle configurations in [2]. Recently a kinodynamic metric based on tipover stability to plan paths on rough terrain was presented in [3] while in [4] tipover stability was used for a decoupled posture and kinematic control of the Hylos robot. The tipover stability was also used as a metric for path planning problem in [13, 14]. However we show later in this paper there are configurations of the robot which have high posture/tipover stability but almost nil velocities or accelerations that satisfy contact and slip constraints simultaneously. That a purely posture based stability

Arun.K.Singh(arunkumar.singh@research.iiit.ac.in)K.Madhava Krishna (mkrishna@iiit.ac.in) and Vijay Eathakota (eathakota.vijay@).iiit.ac.in are with the Robotics Research Lab IIIT-Hyderabad, India

criterion such as tipover does not consider constraints due to contact and no slip and hence may not be fully appropriate to evaluate vehicle stability under high speeds is also mentioned in [5]. Although the author in [12] discusses about feasible acceleration apart from posture based stability the developed equations are inherently planar. Denoted in [5] as dynamic and static stability margins these were used by the same authors earlier for a point mass model [6] and a quasi 3D analysis of a rocker bogie in [7] and of a three-wheeled platform in [5]. The point mass model of [6] was later used as a framework for planning paths for fast moving robots in [8]. However a point mass model does not provide for exact vehicle dynamics while reducing the dimension of the problem to 2 where a search needs to be done for only feasible linear velocity and acceleration.

The quasi-3D analysis in [5] makes use of following assumptions and approximations that could make its application cumbersome or limit its applications. Firstly it projects vehicle dynamics onto pitch, roll and yaw plane and analyses them separately. To achieve this it lumps two appropriate wheels into one. This combination of wheels can be achieved for moderately uneven terrain where the spatial distribution of the contact points does not vary largely with respect to each other. However if two wheels are at largely different heights relative to each other, the framework does not provide information about the calculation of the spatial location of the lumped wheel and hence can affect moment calculations. Another quintessential feature of [5] is the use of analytical functions relating the pitch and roll angles with respect to the path and terrain parameters. Such analytical functions would be possible for simple cases e.g. when the vehicle is traversing a path on a constant slope terrain. For a general 3D terrain, such functions if at all possible would be very difficult to compute. Moreover the rotation matrix of the vehicle is assumed to be known and not derived from the vehicle's evolution on the terrain by computing wheel ground contact points. Thereby it is not possible to immediately use the framework for a planning application wherein it is necessary to compute the traversability of terrain ahead by evolving the vehicle and predicting its posture.

This paper draws upon the notion of computing feasible set of velocities and accelerations as in [5] but differs and thus contributes in the following fashion. Firstly it provides a framework of computing the complete 3D posture of the vehicle by evolution of the vehicle on a fully 3D terrain through CC steer paths [9]. This it does by solving a set of sixteen non-linear equations in sixteen variables unlike

seven linear equations (which would be nine in case of four wheels) used in [5], the framework for which is given in section II. Secondly as a consequence of this the no slip and contact constraints have a fully three dimensional expression that results in determining the feasibility of a location based on an ordered tuple of linear and angular velocities and accelerations than merely linear velocity components in previous approaches. Thirdly since the vehicle posture is being predicted by evolution the framework is immediately amenable within both motion planning and reactive navigation frameworks. Particularly in this effort we make use of the Dynamic Window approach [10] and extend it to a fully 3D framework where in the next best node is computed as that which evaluates a metric the best. The metric used to evaluate a node location couples both the traversability of that location captured through number of ordered pairs of feasible angular and linear accelerations, denoted by *FAC (Feasible Acceleration Count)* and the distance towards the goal from that location denoted by *d*. The coupling takes the form of *FAC/d* since the aim is to maximize the count of the acceleration set and minimize the distance. In our earlier efforts we have shown that a metric of the form *V/t* evaluates and performs better than a metric such as $\alpha V - \beta t$ when the aim is to maximize *V* and minimize *t* [11]. Fourthly comparisons with point mass based motion planning shows the advantages of this current effort, where the point mass model ends up choosing paths of much less dynamic stability than a fully 3D analytical model.

The rest of the paper has been organized as follows: Section II gives the terrain representation information and derivation of equations to determine the posture of the vehicle at a given point on the terrain. Section III derives the vehicle dynamics considering the posture information derived in section II. Section IV describes the concept of feasible and infeasible point on a terrain. Section V describes the dynamic window approach and the proposed path planning methodology. The Simulation results are discussed in Section VI.

II. POSTURE DETERMINATION

A. Terrain Representation and Posture Determination

We assume here that the terrain equation can be represented in the form

$$r = f(p, q) \tag{1}$$

The goal of the posture determination is to compute roll (β), pitch (γ),z coordinate of the centre of the mass and wheel ground contact points in the global reference frame given position (x, y) and heading (α) of the robot.

Posture determination of a car-like vehicle is an indeterminate problem because any vehicle having wheels greater than three is statically indeterminate. The physical interpretation of this indeterminacy is that it cannot be ensured that all wheels touch the ground at all instants. We resolve this problem by introducing a compliance model for one leg and the rigid model for the rest of the three legs. In

the compliant model leg length is taken to be an unknown variable which resolves the indeterminacy problem.

To this effect consider a generic four-wheeled vehicle shown in figure.1. *{O}* represents the global reference frame and its origin is denoted by *O*. *{L}* represents the reference frame having the same orientation as the global frame and attached to the centre of the mass of the chassis *G*. We also attach another reference frame *{G}* (not shown in the figure) at the centre of the chassis such it moves along with the chassis and takes the same orientation as the chassis. We will refer to it as the body reference frame. *Ci* represents the contact point of the *ith* wheel. $\vec{P}_{OG}$ represents the vector from the origin of the global reference frame to the centre of mass of the chassis . $\vec{P}_{Oci}$ represents the position vector to the *ith* wheel contact point. $\vec{P}_{OG}$ and $\vec{P}_{Oci}$ are described in the reference frame *{O}* . $\vec{P}_{gci}$ represents the vector from the centre of the chassis to the wheel ground contact frame described in the reference frame *{L}*.

The holonomic constraint pertaining to the geometry of the vehicle can be written as

$$\vec{P}_{OG} + \vec{P}_{gci} = \vec{P}_{Oci} \tag{2}$$

where $\vec{P}_{gci} = \vec{r_f} + \vec{r_h}$

$\vec{r_f} = R[\frac{(2.5-i)}{|2.5-i|}(h) \quad \delta w \quad 0]^T, \forall\{i = 1,2,3,4\}$

$\vec{r_h} = R[0 \quad 0 \quad -(d_{ri} + r)]^T \forall\{i = 1,2,3\}$ (rigid legs).

$\vec{r_h} = R[0 \quad 0 \quad -(d_{ci} + r)]^T \forall\{i = 4\}$ (compliant leg)

$(2.5 - i)$ has been incorporated to ensure proper sign of half width h corresponding to each vertex of the chassis. w is half breadth of the chassis, d_{ri}, d_{ci} are the leg lengths of rigid and compliant legs respectively ,$\delta = \begin{cases} -1, i = 1,4 \\ 1, i = 2,3 \end{cases}$
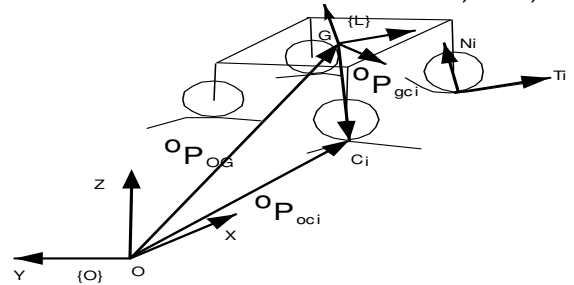

Figure.1 A car-like vehicle.

R is the rotation matrix describing the orientation of the body *{G}* with respect to *{L}*

Hence considering the origin of the global reference frame as (0,0,0),(2) reduces to

$$[x \ y \ z]^T + \vec{r_f} + \vec{r_h} = [x_{ci} \quad y_{ci} \quad z_{ci}]^T \tag{3}$$

Considering a car like vehicle for which yaw will be aligned with the path tangent, α can be taken as a known parameter. Hence for a given (x, y) of the chassis, equation (3) written for all the four wheels will comprise of 12 equations with 16 variables. They are z coordinate of the chassis centre of mass, the roll angleβ, pitch angle γ, 12 wheel ground contact points and the length of the compliant leg. However wheel ground contact points (x_{ci}, y_{ci}, z_{ci}) are related through the surface equation as

$$z_{ci} = f(x_{ci}, y_{ci}) , \ \forall\{i = 1,2,3,4\} \tag{4}$$

(3) and (4) in combination represents 16 non-linear equations in 16 variables which can be solved to obtain uniquely the posture and contact point variables and the compliant leg length. In our work we use MATLAB's FSOLVE routine to solve the above non-linear equations. The convergence or non convergence of the above non-linear equations depicts whether a valid posture is possible on a given point of the terrain or not.

III. VEHICLE DYNAMICS

The philosophy behind deriving the vehicle dynamics is to express the traction and normal forces acting on the wheel ground contact point as a function of linear and angular velocity and acceleration of the chassis. s

A. Traction and normal unit vector derivation

As shown in figure 1 forces act at each wheel-ground contact point are N_i and T_i along the unit vectors $\hat{n}_i$ and $\hat{t}_i$
The normal force unit vector will always be normal to the surface at the wheel ground contact point and can be expressed as

$$[n_{xi}\ n_{yi}\ n_{zi}]^T = \begin{bmatrix} -\frac{fx}{\sqrt{fx^2+fy^2+1}} \\ -\frac{fy}{\sqrt{fx^2+fy^2+1}} \\ \frac{1}{\sqrt{fx^2+fy^2+1}} \end{bmatrix} \quad (5a)$$

$$\begin{cases} fx = \frac{\partial(r-f(p,q))}{\partial p}\Big|p = x_{ci}, q = y_{ci}, r = z_{ci} \\ fy = \frac{\partial(r-f(p,q))}{\partial q}\Big|p = x_{ci}, q = y_{ci}, r = z_{ci} \end{cases} \quad (5b)$$

Once the unit normal vectors are calculated the traction force unit vector can be derived with the help of wheel axis unit vector which in our case has been taken as.

$$\hat{\mu}_i = R[0\ \ 1\ \ 0]^T \quad (6)$$
$$\hat{t}_i = \hat{\mu}_i \times \hat{n}_i \Big/ |\hat{\mu}_i \times \hat{n}_i| \quad (7)$$

B. Velocity and acceleration derivation

We consider non-holonomic class of vehicles in this paper. The velocity(v) of such class of vehicles will be aligned with the longitudinal axis with respect to the body reference frame. Hence the global frame velocity can be represented as
$$[V_x\ \ V_y\ \ V_z]^T = R[v\ \ 0\ \ 0]^T \quad (8)$$
which can be reduced to as
$$V_x = v(c\alpha c\beta) \quad (9)$$
$$V_y = v(s\alpha c\beta) \quad (10)$$
$$V_z = v(-s\beta) \quad (11)$$
So linear acceleration in the global frame can be written as
$$a_x = \dot{v}c\beta c\alpha - vs\alpha c\beta(\dot{\alpha}) - vc\alpha s\beta(\dot{\beta}) \quad (12)$$
$$a_y = \dot{v}s\alpha c\beta + vc\alpha c\beta(\dot{\alpha}) - vs\alpha s\beta(\dot{\beta}) \quad (13)$$
$$a_z = -\dot{v}s\beta - vc\beta(\dot{\beta}) \quad (14)$$
Similarly angular velocities and acceleration in terms of derivative of euler angles can be written as
$$\Omega_x = \dot{\gamma}c\beta c\alpha - \dot{\beta}s\alpha \quad (15)$$
$$\Omega_y = \dot{\gamma}c\beta s\alpha + \dot{\beta}c\alpha \quad (16)$$
$$\Omega_z = \dot{\alpha} - \dot{\gamma}s\beta \quad (17)$$
$$\dot{\Omega}_x = \ddot{\gamma}c\beta s\alpha - \dot{\gamma}\dot{\beta}s\beta s\alpha - \dot{\gamma}\dot{\alpha}c\beta s\alpha - \ddot{\beta}s\alpha - \dot{\beta}\dot{\alpha}c\alpha \quad (18)$$

$$\dot{\Omega}_y = \ddot{\gamma}c\beta s\alpha - \dot{\gamma}\dot{\beta}s\beta s\alpha + \dot{\gamma}\dot{\alpha}c\beta c\alpha + \ddot{\beta}c\alpha - \dot{\beta}\dot{\alpha}s\alpha \quad (19)$$
$$\dot{\Omega}_z = \ddot{\alpha} - \ddot{\gamma}s\beta + \dot{\gamma}\dot{\beta}c\beta \quad (20)$$
Let us discuss the equations (15)-(18) further. In the above equations the only controllable parameter is $v, \dot{v}\alpha, \dot{\alpha}, \ddot{\alpha}$ because for a passive suspension car-like robot only the yaw plane dynamics can be controlled. However the angular velocities and accelerations expressions are coupled and involve contributions from $\dot{\beta}\ \ddot{\beta}\ \ \dot{\gamma}\ \ddot{\gamma}$. To find the values of the roll and pitch velocities and accelerations we do the following. From the motion planning framework presented in section V the pose of the vehicle at the next instant is computed from yaw dynamics and the method described in section II. Then the pitch and roll velocities and accelerations between any two waypoints can be approximated by the following difference equation
$$\dot{\gamma} = (\gamma_{t+\Delta t} - \gamma)/\Delta t \quad (21)$$
$$\dot{\beta} = (\beta_{t+\Delta t} - \beta)/\Delta t \quad (22)$$
$$\ddot{\gamma} = (\gamma_{t-\Delta t} - 2\gamma_t + \gamma_{t+\Delta t})/\Delta t^2 \quad (23)$$
$$\ddot{\beta} = (\beta_{t-\Delta t} - 2\beta_t + \beta_{t+\Delta t})/\Delta t^2 \quad (24)$$
Using the above derivations the vehicle dynamics can be derived as follows:

C. Equations of Motion

The equations of motion for the vehicle can be written as
$$\sum_{i=1}^{i=4} N_i \cdot (\hat{n}_i) + \sum_{i=1}^{i=4} T_i \cdot (\hat{t}_i) = [F_x\ \ F_y\ \ F_z]^T \quad (25)$$
$$\sum_{i=1}^{i=4} \vec{r}_i \times N_i \cdot (\hat{n}_i) + \sum_{i=1}^{i=4} \vec{r}_i \times T_i \cdot (\hat{t}_i) = [M_x\ \ M_y\ \ M_z]^T \quad (26)$$
Where $\vec{r}_i = \vec{P}_{gci} \quad (27)$
$$F_x = ma_x\ (28)\ ; F_y = ma_y\ (29)\ ; F_z = ma_z\ (30)$$
$$M_x = I_{xx}\dot{\Omega}_x (31); M_y = I_{yy}\dot{\Omega}_y\ (32)\ ; M_z = I_{zz}\dot{\Omega}_z\ \ (33)$$
I_{xx}, I_{yy}, I_{zz} are the moment of inertia of the chassis and here a diagonal Inertia matrix has been taken.m is the mass of the vehicle .Equations (25) and (26) can be written in the matrix form as
$$A * C = D \quad (34)$$
$$C = [T_1\ \ N_1\ \ T_2\ \ N_2\ \ T_3\ \ N_3\ \ T_4\ \ N_4]^T$$
$$D = [F_x\ \ F_y\ \ F_z\ \ M_x\ \ M_y\ \ M_z]$$
Matrix A represents an under-constrained matrix and hence to solve for C in terms of D we take the pseudo-inverse of A. So the traction and normal forces as a function of velocity and acceleration can be written as

$$T_i = a_{i1}ma_x + a_{i2}ma_y + a_{i3}(mg + ma_z) + a_{i4}I_{xx}\dot{\Omega}_x + a_{i5}I_{yy}\dot{\Omega}_y + a_{i6}I_{zz}\dot{\Omega}_z = f_1(v, \dot{v}, \alpha, \dot{\alpha}, \ddot{v}, \ddot{\alpha}), \forall\{i = 1,3,5,7\} \quad (35)$$

$$N_i = a_{i1}ma_x + a_{i2}ma_y + a_{i3}(mg + ma_z) + a_{i4}I_{xx}\dot{\Omega}_x + a_{i5}I_{yy}\dot{\Omega}_y + a_{i6}I_{zz}\dot{\Omega}_z = f_2(v, \dot{v}, \alpha, \dot{\alpha}, \ddot{v}, \ddot{\alpha})\ , \forall\{i = 2,4,6,8\} \quad (36)$$

$a_{i1}, a_{i2}, a_{i3}..a_{in}, \forall\ i = \{1,2..8\}$ are the coefficients of the pseudo inverse matrix of A.

Equations (35) and (36) represent non-linear equations in terms of linear and angular velocity and acceleration. A feasible set of linear and angular accelerations and velocities is defined as one which satisfies the following constraints
$$N_i > 0, \forall i = \{1,2,3,4\}\ \ (37) \qquad |T_i| \leq \rho|N_i|\ \ (38)$$

ρ is the coefficient of friction in(38).Through the above set of equations we obtain a range of feasible linear and angular velocities and accelerations. The existence of one such feasible quadruple depends apart from posture also on the terrain conditions such as the spatial distribution of the contact normals.

Hence for some conditions even when the tip-over/posture stability is high, there may not exist any feasible velocity and acceleration satisfying the no-slip and contact constraint. To illustrate this consider a path over a convex terrain as shown in figure.2 in green.
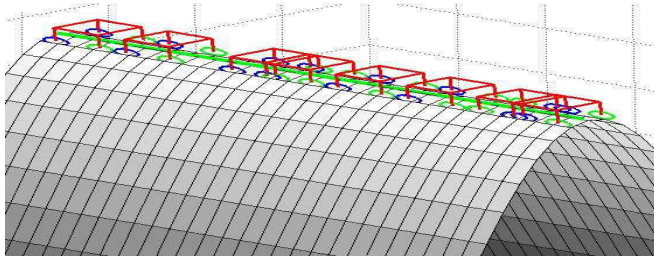
Figure.2 Path on a convex slope

The left and right portions of the vehicle are respectively on two sides of the slope as shown in figure 2. The tip-over metric for the following configuration is shown in figure 3a which shows the normalized tip over metric which is the current tip-over divided by the tip-over value on a flat surface. A constant value of one is because of two reasons, firstly the posture of the vehicle will not change for the path shown in figure.2 and secondly the original tip-over metric is independent of the underlying terrain conditions and depends only on the posture of the vehicle.
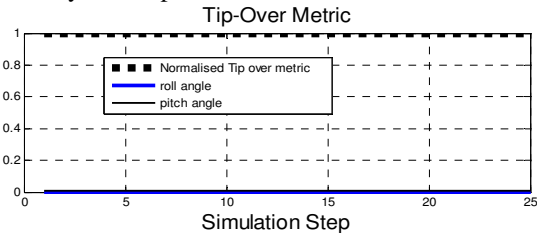

Figure.3a Tip Over vs minimum coefficient metric.

We show in the next section that for these situations no feasible sets of velocities and acceleration exists. Static stability metric like tip-over metric hence is not sufficient to classify a point on a terrain as feasible or infeasible. A point may be statically stable but may not have any possible combination of quadruplet $(v, \dot{v}, \dot{\alpha}, \ddot{\alpha})$ which satisfies the no-slip and contact constraint. So the final decision about a point being feasible or not depends on the existence of feasible velocities and accelerations.

IV. CONCEPT OF FEASIBLE AND INFEASIBLE POINTS

The concept of feasibility and infeasibility of a point on the terrain is defined in two different contexts here: 1. With respect to overall feasibility of a point and 2. Feasibility of a point with respect to the path traversed. The first definition simply says that a point on a terrain is feasible if there exists

any quadruplet $(v, \dot{v}, \dot{\alpha}, \ddot{\alpha})$ which satisfies the no-slip and contact constraint. In the context of definition 1, the path shown in the figure 2 turns out to be infeasible because there exists no velocity and acceleration combination satisfying the constraints at any point of the path. This is shown in figure 3b. However if we relax the no-slip constraint and only enforce the contact constraint we find that the number of feasible velocity is 0.38 times the number of feasible velocities obtain on the flat surface.
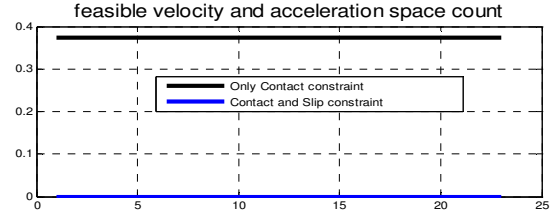

Figure.3b Feasible velocity space plot for the path shown in figure 2

The second definition of feasibility of a point presented here is more conservative and is more appropriate for the motion planning framework described later in the section and is as follows:

Consider two points A and B where the vehicle is currently at point A with velocity $v_A, \dot{\alpha}_A$. Point B is said to be feasible with respect to A if there exists a feasible acceleration $(\dot{v}_A, \ddot{\alpha}_A)$ at A leading to a velocity $(V_B, \dot{\alpha}_B)$ at B such that for the velocity pair $(V_B, \dot{\alpha}_B)$ at B, at-least one acceleration pair of $(\dot{V}_B \ddot{\alpha}_B)$ can be found.. The number of possible such acceleration pairs will be referred to in this paper as feasible acceleration count or *FAC*. The *FAC* is dependent on the velocity possessed by the vehicle.

A. Feasible Velocity and Acceleration search procedure.

As stated earlier a feasible velocity set is a quadruplet $(v, \dot{v}, \dot{\alpha}, \ddot{\alpha})$ such that the contact and no-slip constraints are satisfied. But the velocity terms are dependent on the acceleration values. So the search essentially reduces to searching for the feasible sets of acceleration for the current linear and angular velocity. The search procedure can be summarized as follows:

Given a $v, \dot{\alpha}$ search for $\dot{v}$ in the region $[\dot{v}_{min} \, \dot{v}_{max}]$ and $\ddot{\alpha}$ in the region $[\ddot{\alpha}_{min} \, \ddot{\alpha}_{max}]$ where $\dot{v}_{min}$ and $\ddot{\alpha}_{min}$ are maximum negative accelerations that a vehicle can possess and $\dot{v}_{max}$ and $\ddot{\alpha}_{max}$ are its maximum positive accelerations. Since the vehicle is capable of moving backwards, a negative acceleration can signify a vehicle slowing down or accelerating in the backward direction, depending on the current velocity of the vehicle. *FAC* will depend upon the acceleration limits of the vehicle and hence will vary from vehicle to vehicle. Hence we normalize *FAC* with respect to the value obtained from the flat surface to make it independent of the vehicle characteristics such as maximum acceleration and speed.

V. MOTION PLANNING

In this section we use a method similar to dynamic window approach proposed in [10] in context of motion

planning on uneven terrains. Dynamic window was originally proposed as a reactive collision avoidance technique but we modify it here to generate feasible paths on uneven terrain. Since dynamic window approach directly incorporates the vehicle dynamics and ensures continuity in the velocity space, it proves to be more suitable for uneven terrain motion planning. Moreover being a reactive navigation it finds its merit for online implementation as well. The analogy between original dynamic window approach and the motion planning approach proposed in this approach can be summarized as follows:

In the original dynamic window approach among all possible velocities and accelerations, a kinematically admissible value is found which results in a obstacle free path. In the proposed motion planning framework, a kinematically admissible velocity pair is found for the next instant that is also feasible from the point of view of no slip and contact constraints. The planning algorithm can be summarized as follows:

do while (reach goal)
{

1. for a the current coordinate and state $x_{t_i}, y_{t_i}, \alpha_{t_i} v_{t_i}, \dot{\alpha}_{t_i}$) find all possible n sets of $\dot{v}_t, \ddot{\alpha}_t$ and the corresponding n next nodes $(x_{t_f}, y_{t_f}, \alpha_{t_f} v_{t_f}, \dot{\alpha}_{t_f})$.

2. $for (i = 1:n)$
    Obtain at each $(x_{t_f}, y_{t_f}, \alpha_{t_f})$ the metric M

3. Find the point with minimum M and update that as the current coordinate and repeat step 1-3 until goal is reached.
    end
    }

Here

$$x_{t_f} = x_{t_i} + \int_{t_i}^{t_f} v \cos(\hat{\alpha}) \cos \beta + t(\dot{v} \cos \beta \cos \hat{\alpha} - v \sin \hat{\alpha} \cos \beta (\dot{\alpha}) - v \cos \hat{\alpha} \sin \beta (\dot{\beta})) dt \quad (39)$$

$$y_{t_f} = y_{t_i} + \int_{t_i}^{t_f} v \sin(\hat{\alpha}) \cos \beta + t(\dot{v} \cos \beta \sin \hat{\alpha} + v \cos \hat{\alpha} \cos \beta (\dot{\alpha}) - v \sin \hat{\alpha} \sin \beta (\dot{\beta})) dt \quad (40)$$

$$\hat{\alpha} = \alpha_{t_i} + \dot{\alpha}(t - t_i) + \ddot{\alpha}(t - t_i)^2/2 \quad (41)$$

$$\alpha_{t_f} = \alpha_{t_i} + \dot{\alpha}(t_f - t_i) + \ddot{\alpha}(t_f - t_i)^2/2 \quad (42)$$

Equation (39) and (40) are generalized Fresnel's integral and which ensures generation of kinematically feasible paths. The above equations consider only the yaw plane dynamics since those are the only controllable parameters. The roll and pitch plane motion is ascertained through the approximate method described in section II through equations (21)-(24). It is to be noted that (39) and (40) are not the usual Fresnel's integral for generating CC-steer paths, but are rather modified to take into account the effect of pitch and roll plane motion. In particular it represents the evolution on an average plane formed by the contact points.

Metric M relates FAC to the distance d as $M=FAC/d$ and we show that this metric produces more stable paths than that obtained by considering only the distance. Here d is the distance along the terrain to the goal from the current pose of the robot. This is obtained by discretizing the 3D Euclidean distance from the current pose to the goal at very small

intervals and computing the actual distance along the terrain for each of that interval by projecting any two successive points on the Euclidean distance line onto the terrain below or above as the case might be. An integration of distances along those intervals gives d.

VI. RESULTS AND DISCUSSIONS

The entire frameworks derived in the previous sections were applied to a rigid suspension vehicle model on a planar undulating terrain and on fully 3D terrain. We use $m = 10 \, kg$ and $\rho = 0.7$ in our simulation. The simulation results consist of the following major parts (i). Analysis of the paths produced by only distances metric and metric M. (ii) Comparison of the vehicle's stability along the planned paths from the view point of Tip-Over and FAC. (iii) Affect of velocity on stability of the vehicle. (iv) Comparison of planning effectiveness with full vehicle and point mass model. Simulations were performed on two different types of terrains. The first terrain is a complete 3D surface for which the surface contact normal can be in any arbitrary direction in space, while for the second terrain the surface contact normal are constrained to lie in a plane($X - Y$ in this case). We refer to the second type of terrain in this paper as "planar terrain". Since all the paths generated evolve with different velocity and takes different time to converge to the goal, all the results are plotted by taking X coordinate of the path along the X-axis of the plots

A. Analysis between only distance based and metric M based paths

It can be seen from figure 4 and 5 that distance only metric and metric M produces significantly different paths. This arises because the former searches for waypoints which have larger FAC count. So while distance only metric produces shorter path, metric M produces more stable paths in terms of FAC. The bifurcation between the distance metric path and the metric M based path for the planar terrain occurs at($x = 0.62, y = 6.02$)(fig 4). Similar observations can be made for the path obtained on fully 3D terrains as well, shown in figure.5 where the bifurcation occurs at($x = -11.6, y = 9.71$). To understand the cause of bifurcation note the FAC plot in figures 6a, 6b and figures 7a and 7b (green line). The comparison is between FAC of 6a and 6b and between that of 7a and 7b Prior to the bifurcation point it can be seen that the FAC for both distance and metric M based paths were almost the same. From that point onwards metric M based path continues to move along the direction having higher FAC and a distinct difference in FAC can be seen at the point of bifurcation (circled portion). It must be noted that the forward evolution for the distance metric based paths are also done through feasible linear and angular velocities and accelerations. The difference in both the parts arises only due to the metric used for selecting the next instant nodes.

The metric used for motion planning in this paper makes the algorithm a greedy one. It finds the node that evaluates M the best for the next instant. However the algorithm does

not include information about the conditions ahead of the nodes considered at the next instant. In that sense while it would move to the node with a higher *FAC* for the next instant when compared with distance only metric, this action need not always result in nodes with higher *FAC* when compared with distance only metric for all instances in future as well. For-example from *FAC* plot in figures 6a and 6b, the distance metric based path ends in a higher *FAC* than the metric based paths. But on an average meric *M* based path shows superior performance.

Another important observation is that the metric *M* based path for both planar and 3D terrain tries to align itself with the surface gradient. This agrees with the common intuition that it is easier to move along the gradient of the slope than across it.

B. Comparison of Tip-Over and FAC as stability metric.

Figure 6a and 7a compares normalized tip-over metric and normalized *FAC* for distance only metric based path obtained on planar and 3D terrain respectively while 6b and 7b does the same for the metric M based path. An important observation that arrives from the plot is that even at places where tip–over metric is well above zero, the *FAC* is found to be very close to zero as can be seen from figure 6a and 7a which further reiterates the drawback of using only Tip-Over as a stability metric in the planning process.

C Affect of Velocity on Vehicle stability

The linear velocity plots for distance *M* metric based paths for both planar and 3D terrains are shown in figures 8a and 9a respectively. The negative velocity in the plot is due to the fact that the vehicle model used in the simulation is not constrained to move only in the forward direction. The important thing to note is that linear velocity profile is significantly smooth ensuring the continuity in velocity space. Figure 8a and 9a also shows the velocity limit curves which represent the maximum permissible velocity at that particular instant. The velocity profile of the vehicle is bounded by the velocity limit curve and should always be less than the maximum limit.

As stated earlier *FAC* depends upon the current velocity of the vehicle and hence is a velocity dependent metric. This is illustrated in the figure 8-9 for the planar terrain and 3D terrain respectively. In particular *FAC* is related to the difference between the instantaneous velocity and its maximum limit. The minimum distance between the velocity and its limit curve corresponds to the minimum of the *FAC* curve which is highlighted in figure 8 and 9. However the sensitivity of *FAC* with difference of the velocity and its limit curve is not constant. When both the curves are significantly separated, slight changes in the difference affects *FAC* less than the changes in the difference when the velocity and its limit curve are close.

D. Comparison between point mass model and full Vehicle model

To elucidate the advantage of the full vehicle model over the point mass model, separate paths are generated based on the two models which are shown in figure 10. The equations for

the point mass model were taken from [6]. Figure 11 shows the *FAC* for the point mass model and for the full vehicle model evaluated on the trajectory generated by the point mass model. It can be seen the *FAC* for the full vehicle is more conservative going to zero even at places where the point mass model is showing a high *FAC*. The reason for this being that for the full vehicle model, the no-slip and contact constraints are evaluated for each wheel ground contact point, while the point mass model transfers the wheel ground normal and traction forces to the centre of mass, sums them to get the resultant normal and traction force and then apply the no-slip and contact constraints on the resultant force. Also point mass neglect forces due to angular velocity components. So it is possible for the resultant force to satisfy the no-slip and contact constraint even when all the individual components do not satisfy them individually.
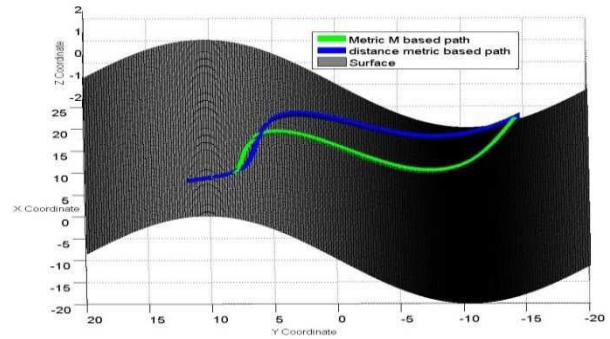

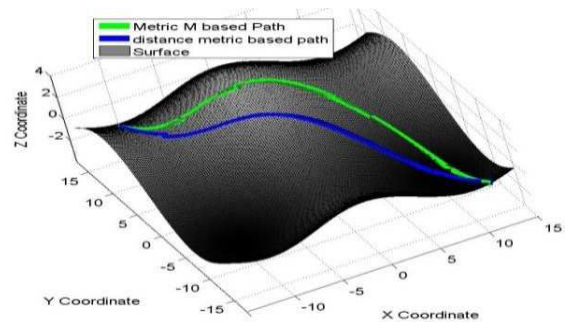Figure.4 Final paths obtained on planar terrain.

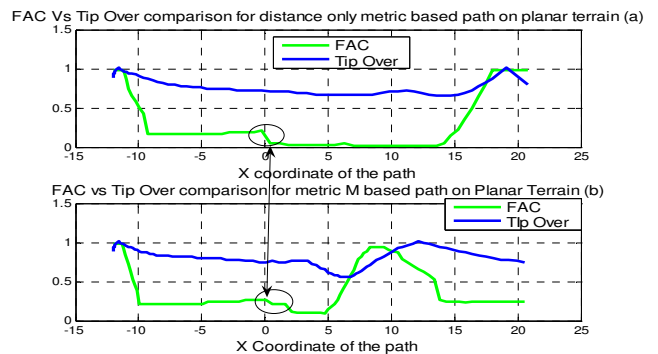Figure.5 Final paths obtained on fully 3D terrain.

Figure.6 Tip over Vs FAC plot for the paths obtained on planar terrain.
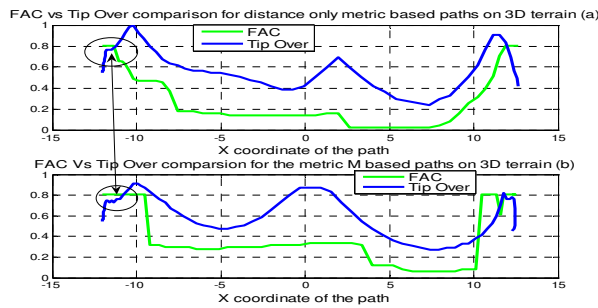
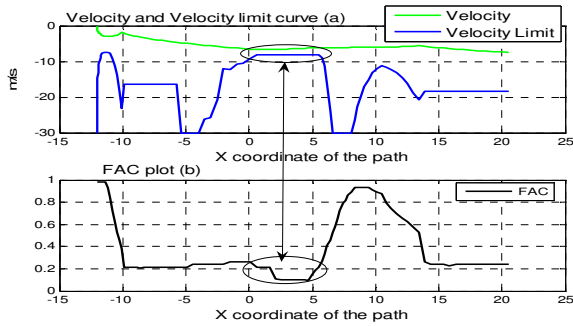Figure.7 Tip-Over and FAC plots for paths obtained on 3D terrains

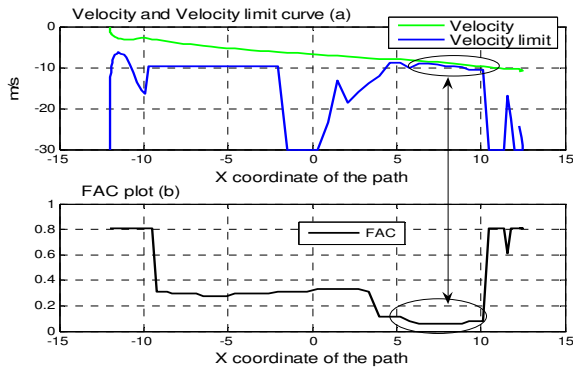Figure.8 plot of linear Velocity for metric M based path on planar terrain

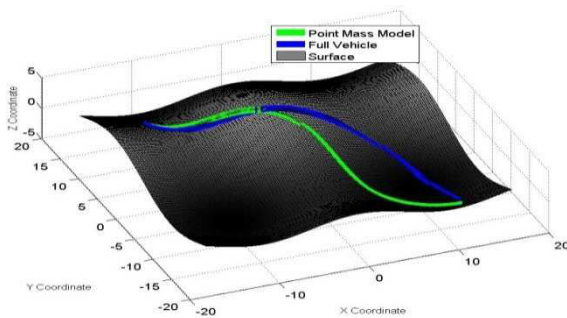Figure.9 plot of linear Velocity for metric M based path on 3D terrainssssss

Figure 10 paths for the point mass and full vehicle model

VII. . CONCLUSIONS

In this paper we proposed a novel physics based framework for motion planning of rovers on uneven terrain. The framework enables determination of posture of a car-like vehicle in 3D and derivation of contact and no-slip constraints in terms of linear and angular velocities and acceleration. A new definition for selection of feasible waypoints in the context of motion planning was introduced

in terms of feasible acceleration count or FAC. FAC was shown to be a more conservative for vehicle stability over tip-over for planning purpose. A novel metric was proposed for best node selection in the planning process which produces more stable paths than that obtained by distance only metric

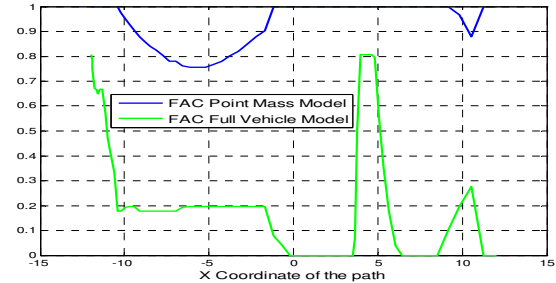Future work is related to working towards extending the framework to reconfigurable vehicles.

Figure.11 FAC comparison between the point mass and full vehicle model

REFERENCES

[1] Papadopoulos E.G , Rey D.A "A new measure for tip-over stability margin for mobile manipulators " in *Proc of International Conference on Robotics and Automation ICRA -1996* pp 3111-3116

[2] D.A .Rey and E.G.Papadopoulos," The force angle stability measure of tip-over stability margin for mobile manipulatorion", *Vehicle System Dyanmics,* vol 32 pp29-48 2000.

[3] J.V.Miro,G Dumonteil,Ch.Beck,GDissanayake, " Kino-dynamic metric to plan stable paths on rough terrains" to appear in *International Conference on Intelligent Robot and Systems IROS 2010,Taiwan*

[4] G. Besseron, Ch. Grand, F. Ben Amar and Ph. Bidaud, "Decoupled control of the high mobility robot Hylos based on a dynamic stability margin**",***IEEE/RSJ Intl Conf on Robots and Systems*, 2435-2440, IROS 2008

[5] M. Mann, Zvi Shiller " Dynamic Stability of offroad vehicles :A quasi-3D analysis" in *Proc of International Conference on Robotics and Automation Pasadena* 2008 CA USA pp 2301-2306.

[6] Shiller, "Obstacle Traversal for Space Exploration", 989-995, *ICRA 2000*

[7] Moshe Mann, Zvi Shiller "Dynamic Stability of a Rocker Bogie Vehicle: Longitudinal Motion" *in Proc of International Conference on Robotics and Automation ICRA 2005* Spain pp-861-866**.**

[8] Karl Iagnemma, Shingo Shimoda, and Zvi Shiller, "Near-Optimal Navigation of High Speed Mobile Robots on Uneven Terrain", *in Proc of International Conference on Intelligent Robots and Systems IROS 2008* Nice, France pp *4098-4103*

[9] T Fraichard and A Scheurer, "From Reeds and Shepp to Continuous Curvature Paths", *IEEE Trans on Robotics*, 20(6), 2004 pp 1025-1035

[10] D. Fox W Burgard Sebastian Thrun " The dynamic window approach for collision avoidance" in *IEEE Robotics and Automation* vol-4 No 1 1997 pp 23-33

[11] Rahul Sawhney, K Madhava Krishna and K Srinathan, "On Fast Exploration in 2D and 3D Terrains with Multiple robots", in *Proc of Autonomous Agents and Multi-Agent Systems (AAMAS), 2009*

[12] Cherif M,"Motion Planning for all terrain vehicles: a physical modeling approach for coping with dynamic and contact interaction constraints" *in IEEE Transactions on Robotics and Automation* April 1999, Volume 15 issue 2 pp 202-218

[13] David Bonnafous, Lacroix S and Simeon T , "Motion generation for a rover on rough terrains" in *Proc of International Conference on Intelligent Robots and Systems IROS-2001* pp-784-789

[14] Kubota T, Kuroda Y, Kunii Y, Yoshimitsu T, " Path planning for a newly developed microver" in *Proc of International Conference on robotics and Automation ICRA -2001*.pp-3710-3715.